Journal of Solid State Chemistry 186 (2012) 54–57

Contents lists available at SciVerse ScienceDirect

Journal of Solid State Chemistry

journal homepage: www.elsevier.com/locate/jssc

Synthesis, structure, and electronic structure of $CsAgGa_2Se_4$

Dajiang Mei [a,b,c], Wenlong Yin [a,b,c], Kai Feng [a,b,c], Lei Bai [a,b], Zheshuai Lin [a,b], Jiyong Yao [a,b,*], Yicheng Wu [a,b]

[a] Center for Crystal Research and Development, Technical Institute of Physics and Chemistry, Chinese Academy of Sciences, Beijing 100190, PR China
[b] Key Laboratory of Functional Crystals and Laser Technology, Chinese Academy of Sciences, Beijing 100190, PR China
[c] Graduate University of Chinese Academy of Sciences, Beijing 100049, PR China

ARTICLE INFO

Article history:
Received 23 August 2011
Received in revised form
31 October 2011
Accepted 6 November 2011
Available online 15 November 2011

Keywords:
Chalcogenide
Synthesis
Crystal structure
Band structure

ABSTRACT

The new metal chalcogenide $CsAgGa_2Se_4$ has been synthesized by means of the reactive flux method. It crystallizes in the space group $P2_1/c$ of the monoclinic system with cell dimensions of $a=11.225(2)$ Å, $b=7.9443(16)$ Å, $c=21.303(4)$ Å, $\beta=103.10(3)$, $V=1850.3(6)$, and $Z=8$. The structure contains two-dimensional $^2_\infty[AgGa_2Se_4]^-$ layers separated by Cs^+ cations. The $^2_\infty[AgGa_2Se_4]^-$ superlayer possesses a novel chain–sublayer–chain structure: a $^2_\infty[Ag_2GaSe_6]^{7-}$ sublayer, composed of $^1_\infty[AgGaSe_4]^{4-}$ chains that are further connected by Ag^+ ions, is sandwiched by parallel $^1_\infty[Ga_3Se_8]^{7-}$ chains to generate the $^2_\infty[AgGa_2Se_4]^-$ superlayer. From a band structure calculation, the orbitals of all atoms have contributions to the bottoms of conduction bands, but the band gap is mainly determined by the 4*s*, 4*p* orbitals of Ga and Se.

© 2011 Elsevier Inc. All rights reserved.

1. Introduction

The ternary $M/M'/Q$ (M=coinage metal, M'=Al, Ga, In, Q=S, Se, Te) chalcogenides have been widely studied for their diverse structures and potential applications in nonlinear optics, solar energy conversion, etc. [1–5]. In contrast, research on the addition of an alkali metal to the ternary $M/M'/Q$ system has been very limited [6–8]. Introducing the strong electrostatic $A-Q$ (A=alkali metal) interactions in the covalently bonded $M-M'-Q$ framework could not only reduce the structure dimensionality from three-dimensional framework to two-dimensional layers or one-dimensional chains, but also alters the electronic structure and physical properties, such as the optical band gap.

So far, $Na_xCu_{1-x}In_5S_8$ ($0<x<1$), $NaAgGa_6Te_{10}$, $K_2CuIn_3Se_6$, $K_2CuGa_3Se_6$, $K_2AgIn_3Se_6$ are the only compounds known in this quaternary $A/M/M'/Q$ (A=Na, K, Rb, Cs; M=coinage metal, M'=Al, Ga, In, Q=S, Se, Te) system [6–8]. $Na_xCu_{1-x}In_5S_8$ ($0<x<1$) adopts the Al_2MgO_4 structure with the optical properties strongly dependent on the value of x. $NaAgGa_6Te_{10}$ adopts a three-dimensional structure composed of $AgTe_4$ and $GaTe_4$ tetrahedra with Na^+ in cavities. The isostructural $K_2CuIn_3Se_6$, $K_2CuGa_3Se_6$, and $K_2AgIn_3Se_6$ can be viewed as a stack of alternate anionic $[MM'_3Se_6]^-$ (M=Cu, Ag; M'=Ga, In) superlayers and K^+ cationic layers. No compounds with the large alkali metal, namely Rb and Cs, were reported in this system. It has been shown that the size of alkali metal has a significant influence on the crystal structures [9–11]. Thus we carried out an exploration in the $A/M/M'/Q$ system, focusing on the larger alkali metals, and successfully discovered a new member in this family, $CsAgGa_2Se_4$, which contains $^2_\infty[AgGa_2Se_4]$ layers with a novel chain–sublayer–chain structure. In this paper, we report the synthesis, structure, and electronic structure of $CsAgGa_2Se_4$.

2. Experimental section

2.1. Single-crystal growth

In the first step, ternary $AgGaSe_2$ was prepared from high purity constituent elements by the high temperature solid-state synthesis technique. The starting materials were Ag (Sinopharm Chemical Reagent Co., Ltd., 99%), Ga (Sinopharm Chemical Reagent Co., Ltd., 99%), and Se (Sinopharm Chemical Reagent Co., Ltd., 99.9%), which were stored in an Ar-filled glovebox. The elements were loaded in the required stoichiometry into a silica ampule and sealed at a residual pressure of $<10^{-3}$ Pa and then reacted at 900 °C for 2 day.

Both binary metal polychalcogenides and metal halides could be used as reactive fluxes [12–16]. In this study, CsI was chosen for the reactive flux. The as-prepared $AgGaSe_2$ powder was mixed with the CsI (Sinopharm Chemical Reagent Co., Ltd., 99%) in the molar ratio of 1:2 and then loaded into a silica tube under an Ar

* Corresponding author at: Center for Crystal Research and Development, Technical Institute of Physics and Chemistry, Chinese Academy of Sciences, Beijing 100190, PR China. Fax: +86 10 82543725.
E-mail address: jyao@mail.ipc.ac.cn (J. Yao).

0022-4596/$ - see front matter © 2011 Elsevier Inc. All rights reserved.
doi:10.1016/j.jssc.2011.11.014

atmosphere in a glovebox, which was sealed under 10^{-3} Pa atmosphere and then placed in a computer-controlled furnace. The samples were heated to 800 °C in 20 h and kept at that temperature for 48 h, then cooled at a slow rate of 4°C/h, and finally cooled to room temperature. The product consisted of yellow crystals of $CsAgGa_2Se_4$, which were manually selected for structure characterization. Analyses of the crystals with an EDX-equipped Hitachi S-3500 SEM showed the presence of Cs, Ag, Ga, and Se in the approximate molar ratio of 1:1:2:4. The crystals are stable in air.

2.2. Structure determination

Single-crystal X-ray diffraction data were collected with the use of graphite-monochromatized Mo $K\alpha$ (λ=0.71073 Å) at 93 K on a Rigaku AFC10 diffractometer equipped with a Saturn CCD detector. Crystal decay was monitored by re-collecting 50 initial frames at the end of data collection and no detectable crystal decay was observed. The collection of the intensity data was carried out with the program Crystalclear [17]. Cell refinement and data reduction were carried out with the use of the program Crystalclear [17], and face-indexed absorption correction was performed numerically with the use of the program XPREP [18].

The structure was solved with Direct Methods implemented in the program SHELXS and refined with the least-squares program SHELXL of the SHELXTL.PC suite of programs [18]. The final refinement included anisotropic displacement parameters. The program STRUCTURE TIDY [19] was then employed to standardize the atomic coordinates. Additional details and structural data are given in Tables 1 and 2 and further information may be found in Supplementary material.

2.3. Band structure calculation

The electronic properties are calculated using the plane-wave pseudopotential method [20] implemented in the CASTEP package [21]. The local density functional (LDA) with a high kinetic-energy cutoff of 650 eV is adopted for all the calculations. The preconditioned conjugated gradient (CG) band-by-band method [22] used in CASTEP ensures a robust efficient search of the energy minimum of the electronic structure ground state. The optimized normal-conserving pseudopotentials [23] in Kleinman–Bylander form [24] for Ag, Cs, Ga, and Se allow us to use a small plane-wave basis set without compromising the accuracy required by our study. The electrons below 4*s* and 5*s* orbitals for sliver and cesium are treated as the core electrons. For gallium the 3*d*, 4*s* and 4*p* electrons are chosen as the valence electrons and for selenium, they are 4*s* and 4*p* electrons. Monkhorst–Pack *k*-point meshes [25] with a density of $(1\times2\times1)$ points in the Brillouin zone of the $CsAgGa_2Se_4$ unit cell are chosen.

Table 1
Crystal data and structure refinement for $CsAgGa_2Se_4$.

	$CsAgGa_2Se_4$
fw	696.06
a (Å)	11.225(2)
b (Å)	7.9443(16)
c (Å)	21.303(4)
β (deg.)	103.10(3)
Space group	$P2_1/c$
V (Å^3)	1850.3(6)
Z	8
T (K)	93 (2)
λ (Å)	0.71073
ρ_c (g/cm^3)	4.998
μ (cm^{-1})	274.04
$R(F)$[a]	0.0479
R_w (F_o^2)[b]	0.1188

[a] $R(F)=\sum||F_o|-|F_c||/\sum|F_o|$ for $F_o^2>2\sigma(F_o^2)$.
[b] $R_w(F_o^2)=\{\sum[w(F_o^2-F_c^2)^2]/\sum wF_o^4\}^{1/2}$ for all data.

Table 2
Selected bond lengths (Å) for $CsAgGa_2Se_4$.

Atoms	Distances	Atoms	Distances	Atoms	Distances
Ag_1–Se_4	2.577(2)	Ga_1–Se_8	2.409(3)	Ga_3–Se_1	2.392(3)
Ag_1–Se_8	2.590(2)	Ga_1–Se_3	2.409(3)	Ga_3–Se_8	2.419(3)
Ag_1–Se_2	2.663(3)	Ga_1–Se_2	2.413(3)	Ga_3–Se_6	2.438(3)
Ag_1–Se_3	2.666(3)	Ga_1–Se_4	2.415(3)	Ga_3–Se_5	2.462(3)
Ag_2–Se_8	2.607(3)	Ga_2–Se_7	2.388(3)	Ga_4–Se_3	2.400(3)
Ag_2–Se_4	2.629(2)	Ga_2–Se_6	2.424(3)	Ga_4–Se_2	2.411(3)
Ag_2–Se_5	2.633(3)	Ga_2–Se_4	2.426(3)	Ga_4–Se_7	2.435(3)
Ag_2–Se_6	2.972(3)	Ga_2–Se_5	2.462(3)	Ga_4–Se_1	2.446(3)

3. Results and discussion

3.1. Structure

$CsAgGa_2Se_4$ crystallizes in a new structure type in space group $P2_1/c$ of the monoclinic system. The asymmetric unit contains two crystallographically independent Cs atoms, two independent Ag atoms, four independent Ga atoms, and eight independent Se atoms. The coordination polyhedra of Cs1 and Cs2 cations are irregular with coordination numbers 8 and 9 and Cs–Se distances in the range of 3.573(2) − 4.260(3) Å. These Cs–Se distances are close to those in $Cs_{10}P_8Se_{20}$ [26] (3.421(6)–4.240(2) Å), $CsAuUSe_3$ [27] (3.604(3)–3.719(3) Å), and $Cs_2Hg_2USe_5$ [28] (3.536(2)–4.224(2) Å). Each Ag atom is coordinated to a slightly distorted tetrahedron of four Se atoms. The Ag–Se distances range from 2.577(2) to 2.972(3) Å, which are comparable to those of $Ba_2Cu_{1.78(7)}Ag_{2.22}Se_5$ [29] (2.552(2)–3.096(2) Å), $BaAg_2SnSe_4$ [30] (2.5670(5)–2.9334(6) Å), $CsTb_2Ag_3Se_5$ [31] (2.6135(8)–2.766(1) Å), and $AgBiP_2Se_6$ [32] (2.762(2)–3.032(3) Å). Each Ga atom is also coordinated to a slightly distorted tetrahedron of four Se atoms. The Ga–Se distances of 2.388(3)–2.462(3) Å are in good agreement with those in $BaGa_4Se_7$ [33] (2.361(2)–2.488(2) Å). Since there are no Se–Se bonds in the structures, the oxidation states of 1+, 1+, 3+, and 2− can be assigned to Cs, Ag, Ga, and Se, respectively.

The crystal structure of the compound can be considered as a stack of alternate anionic ${}^2_\infty[AgGa_2Se_4]$ superlayers and Cs^+ cationic layers (Fig. 1). The structural novelty of $CsAgGa_2Se_4$ derives from the fact that its anionic superlayer is composed of a sublayer sandwiched by parallel chains, as shown in Fig. 2. The two-dimensional ${}^2_\infty[Ag_2GaSe_6]_{7-}$ sublayer is assembled from ${}^1_\infty[AgGaSe_4]_{4-}$ chains that are connected by Ag atoms (Fig. 3(a)) and the parallel ${}^1_\infty[Ga_3Se_8]_{7-}$ chains running above or below the sublayer is composed of $GaSe_4$ tetrahedra (Fig. 3(b)). The structure of $CsAgGa_2Se_4$ is different from that of $K_2AgIn_3Se_6$, which also features a chain–sublayer–chain structure, in two aspects. Firstly, the $In1Se_4$, $In2Se_4$, and $AgSe_4$ are connected to each other by corner-sharing only in the sublayer of $K_2AgIn_3Se_6$ (Fig. 4(a)), while the sublayer in $CsAgGa_2Se_4$ is more complicated in that the edge-sharing $Ag1Se_4$ and $Ga1Se_4$ tetrahedra form ${}^1_\infty[AgGaSe_4]_{4-}$ chains along the *b* direction, which are further connected by the $Ag2Se_4$ tetrahedra by corner-sharing to form the ${}^2_\infty[Ag_2GaSe_6]_{7-}$ sublayer (Fig. 3(a)); Secondly, in the $K_2AgIn_3Se_6$ structure, the chain above or below the sublayer is formed by the corner-sharing $InSe_4$ tetrahedra, as shown in Fig. 4(b), while in the

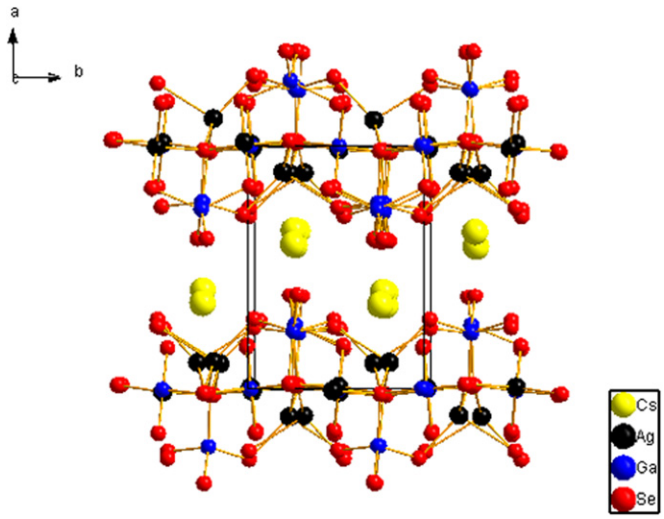

Fig. 1. Unit cell of the $CsAgGa_2Se_4$ structure.

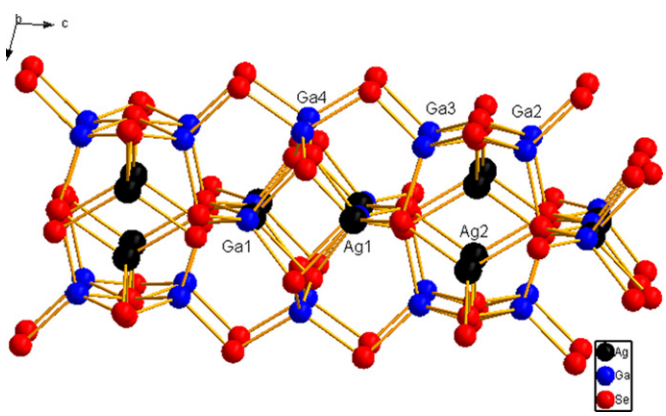

Fig. 2. $^{2}_{\infty}[AgGa_2Se_4]^-$superlayer of $CsAgGa_2Se_4$ structure.

$CsAgGa_2Se_4$ structure, those chains are formed by both corner-sharing and edge-sharing $GaSe_4$ tetrahedra (Fig. 3(b)).

3.2. Band structure calculation

The calculated band structures of the $CsAgGa_2Se_4$ in the unit cell are plotted along the symmetry lines in Fig. 5. It is shown that $CsAgGa_2Se_4$ is a direct gap crystal, and the band gap at G is 1.84 eV, which is larger than the calculated band gaps of $AgGaSe_2$ (1.42 eV) [34] using the same method. It is known that the band gap calculated by LDA is usually smaller than the experimental data due to the discontinuity of exchange-correlation energy. Typically, the difference between the experimental and calculated band gaps is ranged from 0.2 to 0.5 eV for semiconductor systems. Thus, we estimate that the experimental band gap of $CsAgGa_2Se_4$ is about 2.0–2.3 eV, which is consistent with the yellow color of the crystal. In comparison, the $AgGaSe_2$ crystal is red in color, which also indicate that $AgGaSe_2$ possess a smaller band gap than $CsAgGa_2Se_4$.

Fig. 6 gives the total density of states (DOS) and partial DOS (PDOS) projected on the constitutional atoms of the $CsAgGa_2Se_4$ crystal, in which several characteristics can be deduced. (1) The bands localized at -85 eV (not shown) and -14 eV mostly consist by 4*s*, 4*p* orbitals of Ag, 5*s* orbitals of Cs, and 3*d* orbitals of Ga. They do not form the chemical bonding with other orbitals. (2) The orbitals of Cs contribute nothing to the upper region of the valence bands (VB) from -10 eV to 0 eV. These electronic bands

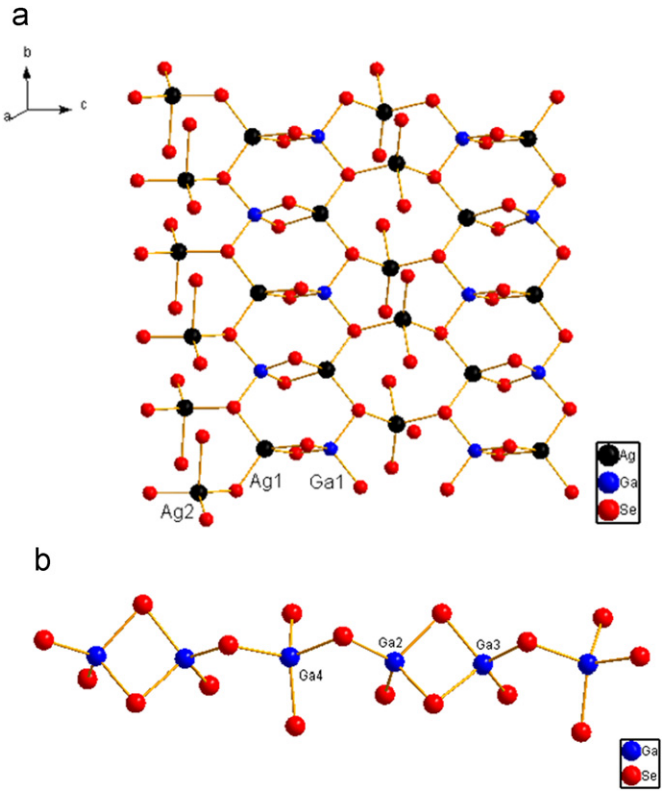

Fig. 3. (a) Sublayer of the $CsAgGa_2Se_4$ structure and (b) the chain above or below the sublayer of the $CsAgGa_2Se_4$ structure

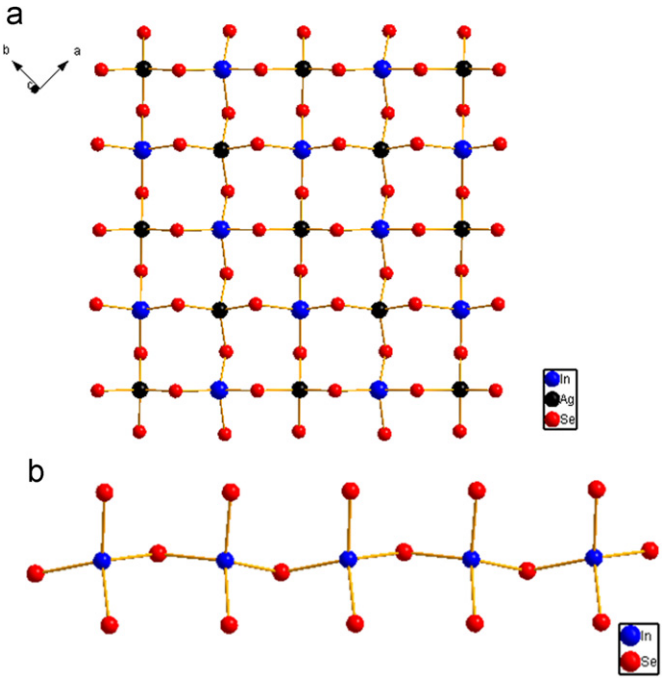

Fig. 4. (a) Sublayer of the $K_2AgIn_3Se_6$ structure and (b) the chain above or below the sublayer of the $K_2AgIn_3Se_6$ structure.

are mainly composed of Ag 4*d*, Ga 4*s* and 4*p* orbitals, as well as Se 4*p* orbitals. The quite large mixture among their states is clearly displayed, revealing that the *Ga–Se*, *Ag–Se* bonds are strong. The very top of the VB from -4 to 0 eV mostly consists of the Se 4*p* orbitals. (3) The orbitals of all atoms have contributions to the bottoms of conduction bands, but compared with $AgGaSe_2$, whose

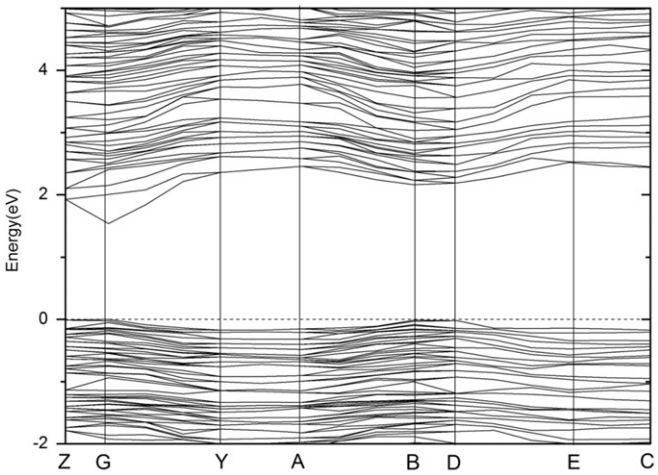

Fig. 5. Band structure of $CsAgGa_2Se_4$ along the lines of high symmetry points in the Brillouin zone. The dash line indicates the VB maximum.

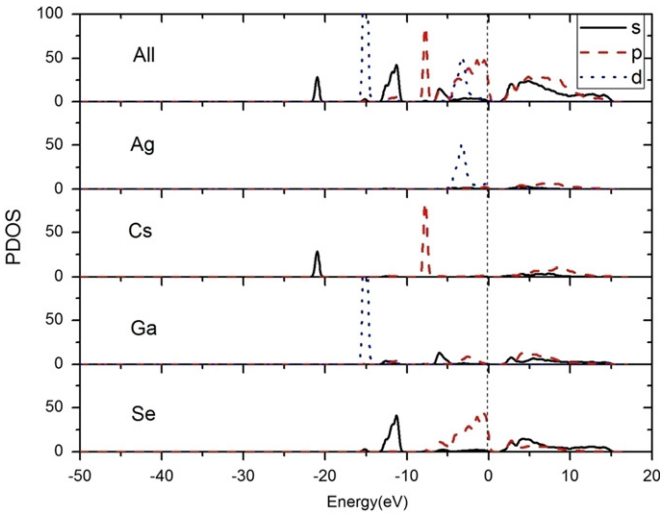

Fig. 6. Partial density of states of $CsAgGa_2Se_4$. The solid, dot-dash, and dash lines are the *s*, *p*, and *d* orbitals, respectively. The broken vertical lines indicate the VB maximum.

band gap is mainly determined by the orbitals of Ag and Se [34], the addition of Cs made the orbital of Ga contribute more than Ag to the band gap. The band gap of $CsAgGa_2Se_4$ is mainly determined by the 4*s*, 4*p* orbitals of Ga and Se. This may be the reason for the increased band gap of $CsAgGa_2Se_4$ compared with $AgGaSe_2$.

4. Conclusions

The new selenide $CsAgGa_2Se_4$ has been synthesized for the first time from the reaction between $AgGaSe_2$ and CsI. It crystallizes in a new structure type in the monoclinic space group $P2_1/c$. The structure contains two-dimensional ${}^2_\infty[AgGa_2Se_4]^-$ layers separated by Cs^+ cations. The novel ${}^2_\infty[AgGa_2Se_4]^-$ layer consists of a ${}^2_\infty[Ag_2GaSe_6]^{7-}$ sublayer sandwiched by ${}^1_\infty[Ga_3Se_8]^{7-}$ chains. The ${}^2_\infty[Ag_2GaSe_6]^{7-}$sublayers is formed by corner and edge-sharing $AgSe_4$ and $GaSe_4$ tetrahedra and the parallel ${}^1_\infty[Ga_3Se_8]^{7-}$ chains above or below the sublayer is composed of corner and edge-sharing $GaSe_4$ tetrahedra. The electronic structure calculation indicates that, compared with $AgGaSe_2$, whose band gap is mainly determined by the orbitals of Ag and Se, the orbital of Ga contribute more than Ag to the optical band gap in $CsAgGa_2Se_4$. Thus the introducing of Cs not only breaks the three-dimensional framework of $AgGaSe_2$ into a two-dimensional structure but also alters the electronic structure.

Supplementary material: The crystallographic data for $CsAgGa_2Se_4$ has been deposited with FIZ Karlsruhe as CSD number 423447. These data may be obtained free of charge by contacting FIZ Karlsruhe at +497247808666 (fax) or crysdata@fiz-karlsruhe.de (e-mail).

Acknowledgments

This research was supported by the National Basic Research Project of China (No. 2010CB630701) and National Natural Science Foundation of China (No. 51072203). Zheshuai Lin acknowledges the Special Foundation of President of Chinese Academy of Sciences.

Appendix A. Supplementary materials

Supplementary data associated with this article can be found in the online version at doi:10.1016/j.jssc.2011.11.014.

References

[1] D.S. Chemla, P.J. Kupecek, D.S. Robertson, R.C. Smith, Opt. Commun. 3 (1971) 29.
[2] G.D. Boyd, H.M. Kasper, J.H. McFee, F.G. Storz, IEEE J. Quan. Electr. 8 (1972) 900.
[3] A. Rockett, R.W. Birkmire, J. Appl. Phys. 70 (1991) R81.
[4] M.A. Contreras, B. Egaas, K. Ramanathan, J. Hiltner, A. Swartzlander, F. Hasoon, R. Noufi, Prog. Photovoltaics Res. Appl. 7 (1999) 311.
[5] M.L. Liu, F.Q. Huang, L.D. Chen, Y.M. Wang, Y.H. Wang, G.F. Li, Q. Zhang, Appl. Phys. Lett. 90 (2007) 072109.
[6] N. Barreau, C. Deudon, A. Lafond, S. Gall, J. Kessler, Sol. Energy Mater. Sol. Cells 90 (2006) 1840.
[7] L. Kienle, H.J. Deiseroth, Z. Kristallogr, New Cryst. Struct. 213 (1998) 19.
[8] H.W. Ma, G.C. Guo, M.S. Wang, G.W. Zhou, S.H. Lin, Z.C. Dong, J.S. Huang, Inorg. Chem. 42 (2003) 1366.
[9] T.K. Bera, J.-H. Song, A.J. Freeman, J.I. Jang, J.B. Ketterson, M.G. Kanatzidis, Angew. Chem. Int. Ed. 47 (2008) 7828.
[10] T.K. Bera, J.I. Jang, J.B. Ketterson, M.G. Kanatzidis, J. Am. Chem. Soc. 131 (2009) 75.
[11] V. Jo, D.W. Lee, H.-J. Koo, K.M. Ok, J. Solid State Chem. 184 (2011) 741.
[12] S.A. Sunshine, D. Kang, J.A. Ibers, J. Am. Chem. Soc. 109 (1987) 6202.
[13] G.B. Jin, S.J. Crerar, A. Mar, T.E. Albrecht-Schmitt, J. Solid State Chem. 179 (2006) 1596.
[14] Y. Liu, L. Chen, L. Wu, Inorg. Chem. 47 (2008) 855.
[15] J.-M. Babo, S. Strobel, T. Schleid, Z. Anorg. Allg. Chem. 636 (2010) 349.
[16] A. Gutzmann, C. Nather, W. Bensch, Inorg. Chem. 43 (2004) 2998.
[17] Rigaku, Crystal Clear, Rigaku Corporation, Tokyo, Japan, 2008.
[18] G.M Sheldrick, Acta Crystallogr. Sect. A: Found. Crystallogr. 64 (2008) 112.
[19] L.M. Gelato, E. Parthé, J. Appl. Crystallogr. 20 (1987) 139.
[20] M.C. Payne, M.P. Teter, D.C. Allan, T.A. Arias, J.D. Joannopoulos, Rev. Mod. Phys. 64 (1992) 1045.
[21] S.J. Clark, M.D. Segall, C.J. Pickard, P.J. Hasnip, M.I.J. Probert, K. Refson, M.C. Payne, Z. Kristallogr. 220 (2005) 567.
[22] A.M. Rappe, K.M. Rabe, E. Kaxiras, J.D. Joannopoulos, Phys. Rev. B 41 (1990) 1227.
[23] J.S. Lin, A. Qteish, M.C. Payne, V. Heine, Phys. Rev. B 47 (1993) 4174.
[24] L. Kleinman, D.M. Bylander, Phys. Rev. Lett. 48 (1982) 1425.
[25] H.J. Monkhorst, J.D. Pack, Phys. Rev. B 13 (1976) 5188.
[26] I. Chung, D. Holmes, D.P Weliky, M.G. Kanatzidis, Inorg. Chem. 49 (2010) 3092.
[27] D.E. Bugaris, J.A. Ibers, J. Solid State Chem. 182 (2009) 2587.
[28] D.E. Bugaris, D.M Wells, J.A. Ibers, J. Solid State Chem. 182 (2009) 1017.
[29] A. Assoud, J. Xu, H. Kleinke, Inorg. Chem. 46 (2007) 9906.
[30] A. Assoud, N. Soheilnia, H. Kleinke, Chem. Mater. 17 (2005) 2255.
[31] F.Q. Huang, J.A. Ibers, J. Solid State Chem. 158 (2001) 299.
[32] M.A. Gave, D. Bilc, S.D. Mahanti, J.D. Breshears, M.G. Kanatzidis, Inorg. Chem. 44 (2005) 5293.
[33] J. Yao, D. Mei, L. Bai, Z. Lin, W. Yin, P. Fu, Y. Wu, Inorg. Chem. 49 (2010) 9212.
[34] L. Bai, Z. Lin, Z. Wang, C. Chen, M.H. Lee, J. Chem. Phys. 120 (2004) 8772.